Analyst

PAPER

View Article Online
View Journal | View Issue

Cite this: *Analyst*, 2014, **139**, 4606

Reagentless uric acid biosensor based on Ni microdiscs-loaded NiO thin film matrix

Kashima Arora,[a] Monika Tomar[b] and Vinay Gupta*[a]

Received 6th June 2014
Accepted 29th June 2014

DOI: 10.1039/c4an01029a

www.rsc.org/analyst

The development of a noninvasive test for uric acid has been the holy grail of uric acid detection research over the last decade. In the present work, a novel matrix comprising of a NiO thin film (a biocompatible material) loaded with Ni microdiscs was prepared on an ITO-coated glass substrate (Ni/NiO/ITO) with the help of RF sputtering for the reagentless detection of uric acid. The bioelectrode was fabricated by immobilizing uricase using a physical adsorption technique on the surface of the Ni/NiO/ITO electrode. The prepared matrix was found to be efficient in sensing biological processes occurring on the surface of the bioelectrode (Ur/Ni/NiO/ITO) in the presence of the analyte (uric acid) to obtain an electronic output. The biosensor exhibits a high sensitivity (431.09 μA mM^{-1}), low K_m value (0.15 mM), high apparent enzyme activity (5.07×10^{-2} units per cm^2), high shelf life (20 weeks) and good selectivity for the detection of uric acid over a wide concentration range (0.05 mM to 1 mM) without any external mediator in the PBS buffer. The obtained results are encouraging for the realization of a reagentless uric acid biosensor with efficient sensing response characteristics.

Introduction

Uric acid is a product of the metabolic breakdown of purine nucleotides in the liver and is the chief nitrogenous component of biological fluids such as urine and blood serum. Estimation of the uric acid concentration in blood has recently become clinically important for the diagnosis of various diseases such as gout, hyperuricemia or Lesch–Nyhan syndrome, arthritis, diabetes, renal, neurological, cardiovascular and kidney-related problems.[1] Thus, precise detection of the uric acid concentration in blood is of significant interest for biomedical applications and requires immediate attention. A number of techniques have been used for the detection of uric acid including amperometric, potentiometric, optical, thermal, and piezoelectric techniques.[2–5] Among them, the enzyme (uricase)-based amperometric biosensor is considered to be the most promising approach as it offers a fast, simple and low-cost detection technique. Several matrices, such as conducting polymers, CNTs, metal nanoparticles, and composite thin films, have been used to immobilize uricase for the fabrication of uric acid biosensors and are summarized in Table 1.[6–9] It may be noted from Table 1 that most of the bioelectrodes exploited for detection of uric acid are found to suffer from certain problems such as a lack of stability, time-consuming, non linear detection range, leaching out of immobilized enzyme, low sensitivity, and higher values of the limit of detection, thereby limiting their application in development of an efficient uric acid biosensor. Recently, metal oxide-based thin films matrices have gained significant attention for biosensing applications because of their biocompatibility, ease of processing, high stability, good sensitivity, excellent selectivity, low detection limit, low cost and the capability of being fabricated on an integrated biochip.[10–13] Among the various matrices, nickel oxide (NiO), which is a p-type and wide band gap (3.7 eV) semiconductor, has attracted immense interest. This matrix by its virtue of natural abundance, low cost, nontoxicity, high chemical stability, biocompatibility, good electron communication feature and high isoelectric point (IEP $\sim$ 10.7) is advantageous in binding biomolecules, which have a low IEP by strong electrostatic interactions. NiO thin films and their composites are efficiently used for the development of various biosensors for estimation of haemoglobin, glucose, metformin, and uric acid.[14–17] However, in all such estimations, either the sensitivity is poor or an external mediator in the PBS solution is used to obtain a redox couple. Despite the fact that Ni has multivalence states (Ni^{2+} and Ni^{3+}), a novel approach is required to activate the electrocatalytic activity of the NiO-based matrix. Since NiO has its own redox couple, it provides direct electron transfer between the redox protein and electrode, which may pave a way towards the realization of a reagentless bioelectrode for the efficient detection of uric acid.

In this study, a reagentless uric acid biosensor has been successfully fabricated using a novel NiO thin film matrix loaded with Ni microdiscs. The biosensing response characteristics of the prepared bioelectrode (Ur/Ni/NiO/ITO) as a function of the uric acid concentration have been studied using

[a]*Department of Physics and Astrophysics, University of Delhi, Delhi 110007, India. E-mail: vgupta@physics.du.ac.in*

[b]*Physics Department, Miranda House, University of Delhi, Delhi 110007, India*

Table 1 Brief summary of the amperometric sensing parameters of the uric acid biosensors reported by various researchers. The corresponding Ni/NiO/ITO electrode is also included for comparison

S.no.	Material	Range (mM)	Sensitivity ($\mu A\ mM^{-1}$)	Response time (s)	Detection limit (mM)	*S*/*N*	Reference
1.	SAM of APTES bis sulfosuccinimide/ITO	0.05–0.58	39.35	50	0.037	3	6
2.	Gold electrode/polystyrene	5×10^{-3}–105×10^{-3}		60			8
3.	Carbon felt based H_2O_2	0.3×10^{-3}–20×10^{-3}	0.25		0.18×10^{-3}	3	21
4.	MWCNT–Ch/ poly(amidoamine)/DNA/ gold electrode	0.5×10^{-3}–100×10^{-3}	43.9×10^{-6}	5	0.07×10^{-3}	3	22
5.	Polyaniline	0.01–0.6	47.2	60	0.01		9
6.	Polyurethane hydrogel	0–2		80–100			2
7.	Screen printed electrode	2×10^{-3}–40×10^{-3}	3.05		0.42×10^{-3}		23
8.	Poly(oaminophenol) C paste electrode	0.1	5	37	3×10^{-3}		24
9.	Pyrolytic C film electrode		61.92		0.03×10^{-3}		25
10.	N Doped graphene	1×10^{-4}–2×10^{-2}			4.5×10^{-5}	3	26
11.	Zn–Ni nanoalloy/graphite	1×10^{-3}–400×10^{-3}			0.2×10^{-3}	3	27
12.	Polyelectrolyte PDDA	1×10^{-3}–60×10^{-3}	50		1×10^{-3}		28
13.	MWCNT/Au nps.	0.01–0.8	44	7	0.01	3	29
14.	3 Amino5-mercapto-124 triazole/GC	40×10^{-6}–0.1		50	0.52×10^{-6}	3	30
15.	Polypyrrole/Pt	7.5×10^{-8}–8.3×10^{-3}			75×10^{-9}		31
16.	Epoxy resin biocomposite	0.025–0.1		12	4.25	3	32
17.	Mol. Imprinted polymer (MIP)	0–1.125	24.72		0.3×10^{-3}	3	33
18.	Ir–C electrode	0.1–0.8	16.60	<45	0.01	6.18	34
19.	Ur-Peroxidase + Amplex red	1×10^{-3}			20×10^{-6}		35
20.	PB nps/MWCNT/PANI/Au composite	0.005–0.8		4	5×10^{-3}	3	36
21.	SAM thiosubstituted nucleobases/Au	1×10^{-3}–500×10^{-3}	0.78	8	1×10^{-3}		37
22.	Ni microdiscs/NiO/ITO matrix	0.05–1	431.09	4	0.03	3	Present work

amperometric and photometric techniques. The reagentless detection of uric acid with enhanced sensing response has been obtained after integrating the Ni microdiscs with a NiO thin film by rf magnetron sputtering.

Experimental

Materials and methods

Uricase, horseradish peroxidase (HRP) (200 U mg^{-1}) and *o*-dianisidine were purchased from Sigma-Aldrich. Anhydrous monobasic sodium phosphate and dibasic sodium phosphate dihydrate were obtained from Sisco chemical, India. Deionized water (resistivity =18.2 MΩ cm^{-1}) was used for preparation of the aqueous solutions.

Measurement and apparatus

For studying the structural properties, X-ray diffraction (XRD) was carried out using a Bruker X-ray diffractometer to identify the crystallographic structure of the prepared matrices of NiO and Ni/NiO. The surface morphology of the film and bioelectrode was studied by scanning electron microscopy (SEM). The photometric assay of the prepared bioelectrodes were performed using a UV-visible spectrophotometer (Perkin Elmer:Lambda 35) to investigate the binding of Uricase onto the electrode surface. Electrochemical measurements were conducted on Gamry potentiostat/galvanostat (Ref 600) using a three-electrode cell containing Ag/AgCl as the reference electrode, platinum (Pt) as the counter electrode and the prepared electrodes (NiO/ITO and Ni/NiO/ITO) as the working electrode in PBS buffer of pH 7.0.

Preparation of solutions

Phosphate buffer saline (PBS) (50 mM, pH 7.0) was prepared by adjusting the proportion of monobasic sodium phosphate and dibasic sodium phosphate solutions, and then adding 0.9% NaCl to the solution. Uricase (1 mg mL^{-1}) and HRP solutions (1 mg mL^{-1}) were freshly prepared in PBS buffer (pH 7.0). Different concentrations of uric acid solution (0.05–1.00 mM) and a solution of *o*-dianisidine (1%) dye were freshly prepared in de-ionized water.

Preparation of NiO thin film and Ni microdiscs/NiO thin film matrices and immobilization of uricase

NiO film of thickness 245 nm was deposited on an ITO-coated corning glass substrate (ITO/glass) using a rf-magnetron

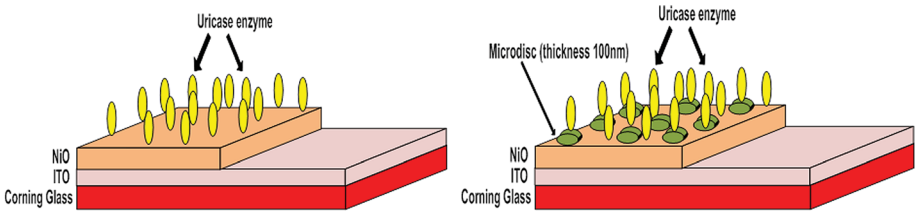

Fig. 1 Schematic of the prepared Ur/NiO/ITO and Ur/Ni/NiO/ITO bioelectrodes.

sputtering technique. A nickel metal target (99.99% pure and 2 inch diameter) was sputtered in a reactive gas mixture (50% O_2 and 50% Ar) at a growth pressure of 30 mT using 40 W rf power without any external substrate heating. ITO-coated corning glass substrates of area 2.0 cm × 0.5 cm was used, out of which a 1.0 cm × 0.5 cm area was masked for the electrical contacts, and the NiO thin film was deposited on the remaining area of 1.0 cm × 0.5 cm of the ITO/glass substrate. A schematic of the sensor structure prepared in the present study is shown in Fig. 1. Microdiscs of Ni of 100 nm thickness were deposited on the surface of the NiO thin film (Ni/NiO/ITO) by rf sputtering through a shadow mask (pore diameter ~ 250 μm), using a Ni target in an 100% Ar atmosphere at a growth pressure of 10 mT and by applying an RF power of 40 W. The electrode without Ni microdiscs (NiO/ITO) was also prepared for comparison with a Ni/NiO/ITO electrode (Fig. 1). Uricase (Ur) enzyme was immobilized on the surface of both electrodes (NiO/ITO and Ni/NiO/ITO) by a physical adsorption technique. A 0.5 cm^2 area of both the electrodes was dipped in a solution of uricase (1 mg mL^{-1}) that was prepared in 50 mM (0.9% NaCl) phosphate buffer saline (PBS). The electrodes were kept overnight for enzyme (Uricase) immobilization, and subsequently washed with a PBS solution and dried under nitrogen flow. A schematic of the immobilization of uricase on the surface of Ni/NiO/ITO matrix is shown in Fig. 2. The prepared bioelectrodes Ur/Ni/NiO/ITO and Ur/NiO/ITO (Fig. 1) were stored at 4 °C when not in use.

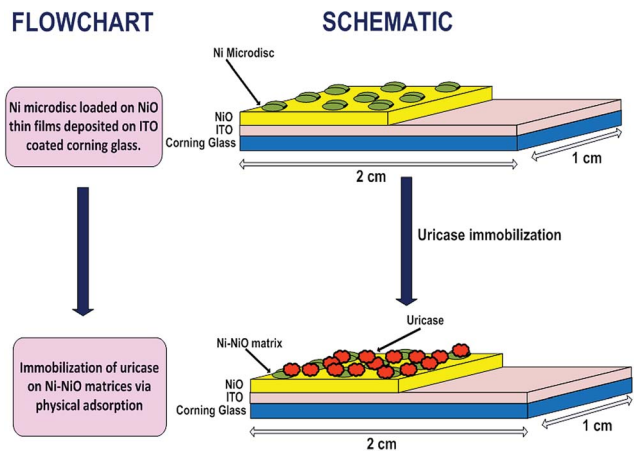

Fig. 2 Schematic and flowchart of the preparation of Ur/Ni/NiO/ITO bioelectrode using immobilized uricase *via* physical adsorption technique.

Results and discussion

NiO/ITO and Ni microdiscs/NiO/ITO matrices deposited by RF sputtering under the optimized growth conditions were found to be smooth and strongly adherent to all the substrates.

Structural property

The as-deposited NiO thin film deposited at room temperature was found to be amorphous and became polycrystalline when annealed in air at a temperature of 100 °C for one hour. The XRD patterns of the NiO and Ni/NiO matrices deposited on the ITO-coated corning glass substrate after post-deposition annealing at 100 °C are shown in the inset of Fig. 3. The XRD pattern of NiO thin films exhibits three well-defined diffraction peaks corresponding to the (111), (200) and (220) planes of NiO, indicating the growth of a polycrystalline thin film (inset of Fig. 3). An additional peak at $2\theta \sim 51.6°$ in the XRD pattern of Ni/NiO matrix corresponds to Ni and confirms the presence of Ni microdiscs on the surface of the NiO thin film matrix.[18]

Optical property

NiO and Ni/NiO matrix were also deposited on a corning glass substrate (without an ITO coating) under similar deposition conditions for optical characterization. The UV-Visible transmission spectra of NiO and Ni/NiO recorded over the wavelength range of 190–1100 nm are shown in Fig. 3. The NiO thin film was found to exhibit relatively low transmission (~65%) in the visible region (Fig. 3), indicating the growth of a metal-rich

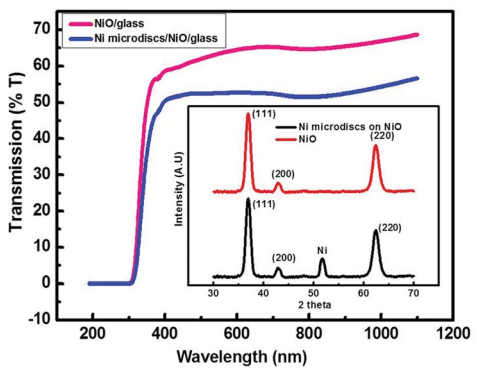

Fig. 3 UV-Visible transmission spectra of NiO/glass and Ni/NiO/glass substrates; Inset shows the X-ray diffraction patterns of NiO/glass and Ni/NiO/glass.

NiO thin film under an oxygen deficient reactive gas environment. It may be noted from Fig. 3 that the optical transmission further decreased to about 50% in the visible region when Ni microdiscs were integrated with NiO thin film. Both thin film matrices showed a sharp fall in the UV region at around 310 nm, corresponding to the onset of a fundamental absorption edge (Fig. 3). The band gap of NiO and the Ni/NiO thin film matrices was evaluated using Tauc plots, and its value was found to be about 3.78 to 3.53 eV, respectively. The value of 3.78 is in agreement with the corresponding value reported for NiO thin film by other workers.[19] However, the value of E_g was slightly reduced to 3.53 eV after integrating with Ni microdiscs.

Surface morphology

The surface morphologies of (i) NiO/ITO electrode and (ii) uricase/NiO/ITO bioelectrode were studied by SEM, and images are shown in Fig. 4(a) and (b), respectively. The surface of the NiO thin film showed a fine homogeneous morphology with uniformly distributed nanosize crystallites [Fig. 4(a)]. The surface morphology became rough after the immobilization of macromolecules of uricase (1 mg mL^{-1}) onto the surface of the NiO/ITO electrode. The uniformly distributed globular structure observed in the SEM image of the surface of uricase/NiO/ITO biosensor [Fig. 4(b)] revealed the successful binding of the enzyme with homogeneous coverage as well as dense loading.

Electrochemical property

NiO/ITO electrode. In our earlier work, the fabrication of a NiO thin film-based uric acid biosensor was reported, in which sensing was carried out in a mediated buffer.[1] For the development of a reagentless NiO based biosensor, the deposition conditions of the NiO thin films were varied so that the redox properties of the NiO matrix could be obtained without using any external mediator in the buffer solution.

The CV response of the NiO/ITO electrode thin film in a reagentless PBS buffer in the potential range from −0.3 to 0.8 V is shown in Fig. 5(a). It may be noted from Fig. 5(a) that well-defined oxidation and reduction peaks are obtained for the Ni^{3+}/Ni^{2+} redox couple in the NiO thin film matrix. It is important to point out that the CV curves obtained for the electrodes having NiO thin films of different thickness (180 nm to 270 nm) are shown in Fig. 5(a). With increasing thickness of the NiO thin film from 180 to 245 nm, the peak oxidation current increases continuously from 27 μA to 50 μA and decreased thereafter with further increases in the thickness (>245 nm) of the NiO thin film (inset of Fig. 5(a)). Therefore, 245 nm thin NiO film was used for the preparation of bioelectrodes for further study.

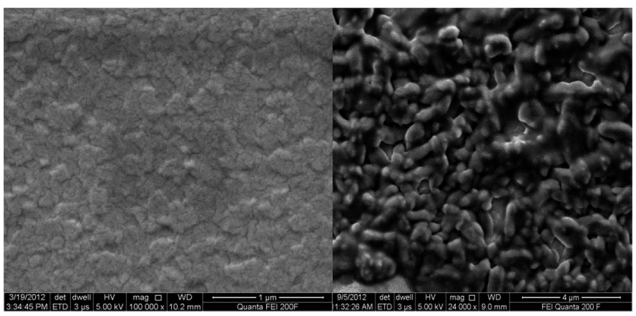

Fig. 4 SEM image of (a) NiO/ITO matrix and (b) uricase immobilized on NiO/ITO.

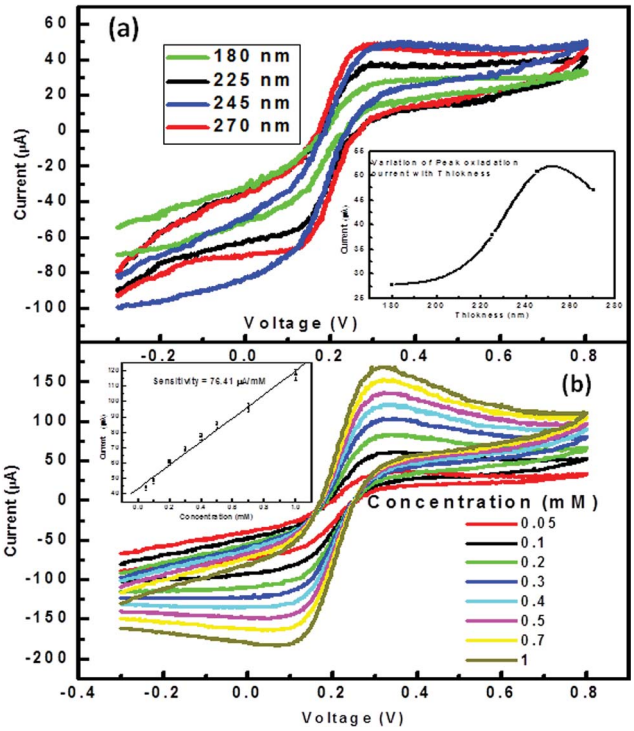

Fig. 5 (a) Cyclic voltammogram of NiO/ITO electrode having different thickness of NiO film, the inset of (a) shows the variation of the peak oxidation current with thickness, (b) amperometric sensing response of Ur/NiO/ITO bioelectrode with an increase in uric acid concentration, the inset of (b) shows the variation of peak oxidation current with the uric acid concentration.

The CV curve, which was obtained after immobilizing uricase on the surface of the NiO/ITO electrode, reflects a decrease in the peak oxidation current from 50 μA to 23 μA. The decrease is due to the non-conducting nature of the macromolecules of uricase.

Fig. 5(b) shows the amperometric sensing response of the Ur/NiO/ITO bioelectrode upon the successive addition of uric acid in the PBS solution. It can be seen that the peak oxidation current of the bioelectrode increases linearly from 35 μA to 169 μA with increasing uric acid concentration from 0.05 to 1.00 mM (inset of Fig. 5(b)) with a correlation coefficient (R) of 0.98, indicating good electrocatalytic behaviour of the NiO matrix. The sensitivity of the Ur/NiO/ITO bioelectrode, as calculated from the calibration curve, was found to be about 76.41 μA mM^{-1}. The obtained results are slightly inferior to the corresponding results by other researchers, who reported uric acid biosensors using external mediators;[20] nevertheless, the reagentless detection in the present study is advantageous.

Ni/NiO/ITO electrode. The CV response of the Ni/NiO/ITO electrode, having Ni microdiscs, were studied in a PBS buffer without any mediator. The corresponding curve obtained for

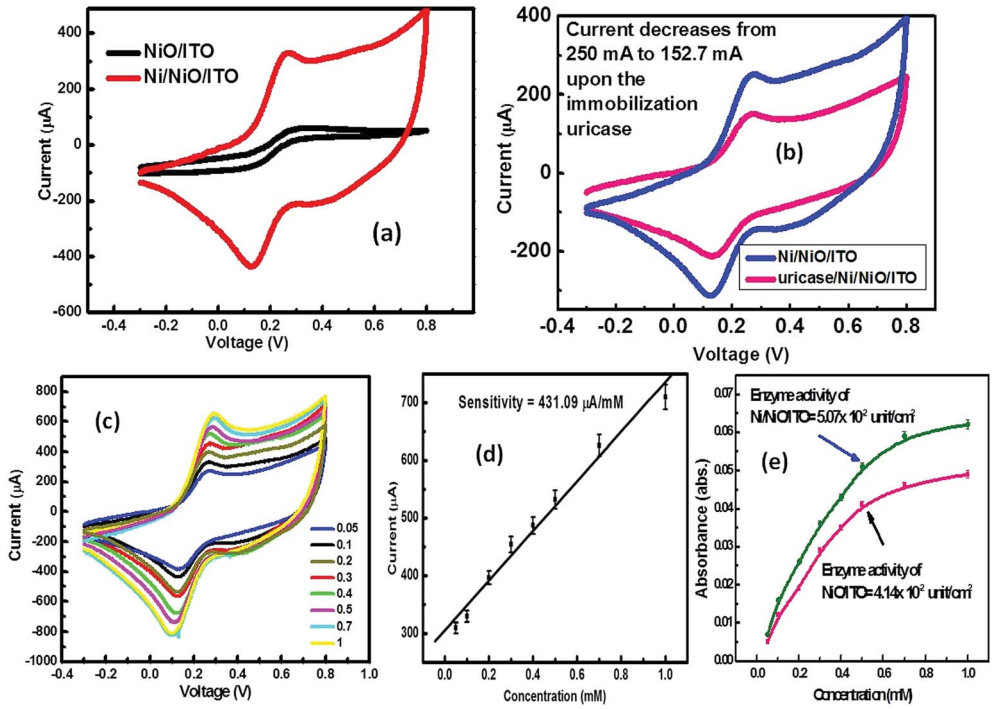

Fig. 6 (a) Cyclic voltammogram (CV) of Ni/NiO/ITO and NiO/ITO electrodes, (b) shows CV of Ni/NiO/ITO electrode and Ur/Ni/NiO/ITO bio-electrode, (c) sensing response of uricase/Ni/NiO/ITO bioelectrode as a function of the uric acid concentration: (i) 0.05 (ii) 0.1 (iii) 0.2 (iv) 0.3 (v) 0.4 (vi) 0.5 (vii) 0.7 and (viii) 1.00 mM, (d) shows the variation of the peak oxidation current as a function of the uric acid concentration and (e) shows the photometric assay of uricase/Ni/NiO/ITO and uricase/NiO/ITO bio-electrodes as a function of the uric acid concentration.

bare NiO/ITO electrode (without Ni microdiscs) is also included in Fig. 6(a) for comparison. A drastic enhancement in the peak oxidation current from 50 μA to 250 μA was observed as a result of the integration of Ni microdiscs with the surface of the NiO/ITO electrode (Fig. 6(a)). The presence of Ni microdiscs provided excess charge carriers for transport *via* the Ni^{3+}/Ni^{2+} redox couple for obtaining a CV curve that showed an enhanced oxidation peak current obtained without any mediator in the buffer. A decrease in the peak oxidation current from 250 μA to 152 μA was observed when uricase was immobilized on the surface of the Ni/NiO/ITO electrode (Fig.6(b)) and was attributed to the non-conducting nature of the macromolecules of uricase.

Amperometric sensing response characteristics: Ur/Ni/NiO/ITO bioelectrode as a function of uric acid

The concentration is shown in Fig. 6(c) in a reagent-free PBS solution. A linear increase in the peak oxidation current from 283 μA to 655.33 μA was observed for the Ur/Ni/NiO/ITO bio-electrode, affected by the increase in the concentration of uric acid from 0.05 to 1.0 mM. The sensitivity of the bioelectrode (Ur/Ni/NiO/ITO) having Ni microdiscs was found to be about 431.09 μA mM^{-1} (Fig. 6(d)), which is much higher compared to the corresponding value (76.41 μA mM^{-1}) obtained for uricase/NiO/ITO bioelectrode. The detection limit was found to be about 0.06 mM. The lower detection limit was calculated using the expression, $3S_{y/x}$/sensitivity, where $S_{y/x}$ is the standard deviation obtained from the peak oxidation current *versus* analyte concentration curve (Fig. 6(d)). The obtained value of sensitivity for the Ni microdisc-based bioelectrode was found to be much higher in comparison to the corresponding value reported for uric acid biosensors by various researchers in the literature [Table 1]. This was attributed to the availability of both the Ni microdiscs and uncovered surface of the NiO thin film, which resulted in the immobilization of uricase and subsequently faster transfer of large amounts of charge carriers from enzyme to electrode.

Michaelis–Menten kinetic parameter (K_m)

The graph of the ratio of the analyte concentration to the oxidation peak current *versus* the analyte concentration (Hanes plot) was plotted and used to evaluate the value of Michaelis–Menten constant (K_m) for both uricase/NiO/ITO and uricase/Ni/NiO/ITO bioelectrodes, and it was found to be about 0.21 and 0.15 mM, respectively. The low value of K_m (0.15 mM) obtained for uricase/Ni/NiO/ITO bioelectrode indicates the high affinity of the immobilized uricase towards its analyte (uric acid), which was attributed to the effective loading of the enzyme due to the high surface area along with high electron communication property of the prepared matrix with a NiO thin film loaded with Ni microdiscs. The bioelectrode having Ni microdiscs (Ur/Ni/NiO/ITO) was also found to attain about 98% of its steady state in less than 5 s, indicating the fast electron communication between the immobilized uricase and the electrode *via* Ni/NiO matrix.

Table 2 Determination and recovery of uric acid in human serum samples using the prepared uricase/Ni/NiO/ITO/glass biosensor

Real sample (serum)	Concentration of uric acid measured (mM)		R.S.D. of developed biosensor ($n = 5$) (%)	Spike (mM)	Concentration of uric acid detected (mM)	Recovery (%)	R.S.D. of developed biosensor ($n = 5$) (%)
	Uricase/Ni/NiO/ITO/glass biosensor	Spectrophotometric method					
1	0.315	0.319	1.5	0.5	0.831	103.2	1.2
2	0.238	0.243	1.2	0.5	0.751	102.6	1.4
3	0.667	0.676	2.3	0.5	1.180	102.6	2.7
4	0.483	0.489	2.5	0.5	0.99	101.4	1.9
5	0.107	0.112	1.7	0.5	0.601	98.8	2.0
6	0.558	0.552	1.3	0.5	1.101	108.6	1.5
7	0.295	0.292	3.1	0.5	0.78	97	2.5
8	0.713	0.717	2.1	0.5	1.214	100.2	1.9
9	0.887	0.883	1.8	0.5	1.39	100.6	2.0
10	0.612	0.608	1.6	0.5	1.11	99.6	1.3

Photometric enzyme assay

To carry out the photometric enzyme assay, both bioelectrodes were dipped separately in 3 mL PBS solution containing 20 μL horseradish peroxidise (HRP), 20 μL *o*-dianisidine dye and 100 μL of analyte (uric acid) at varying concentrations. The difference between the initial and final absorbance of the analyte at $\lambda = 500$ nm was recorded after 2 min, and it is shown in Fig. 6(e) as a function of the uric acid concentration. The uricase enzyme activity increased with increase in the uric acid concentration up to 0.5 mM for both bioelectrodes, and then showed a saturating tendency with further increase in concentration (>0.5 mM). The amount of bound enzyme is determined from the apparent enzyme activity ($a_{\mathrm{enz}}^{\mathrm{app}}$) calculated using the following equation:

$$a_{\mathrm{enz}}^{\mathrm{app}}\left(\mathrm{U\ cm^{-2}}\right) = \frac{AV}{\varepsilon t s} \quad (1)$$

where A is the difference in absorbance of the bioelectrode before and after incubation, V is the total volume (=3.17 $\mathrm{cm^3}$), ε is the millimolar extinction coefficient for *o*-dianisidine ($\varepsilon \sim 7.5$ for at 500 nm), t is the reaction time (2 min), and s is the surface area of the electrode (1.0×0.5 $\mathrm{cm^2}$). The values of the apparent enzyme activity of uricase immobilized on the surface of NiO/ITO and Ni/NiO/ITO electrodes were found to be about 4.14×10^{-2} unit per $\mathrm{cm^2}$ and 5.07×10^{-2} unit per $\mathrm{cm^2}$, respectively. The obtained results clearly indicate that the composite matrix of the NiO thin film loaded with Ni microdiscs provides a better platform for the effective and conformal immobilization of the enzyme; hence, more units of uricase are actively working on its unit surface area. The results in the present work were found to be better in comparison to those reported in the literature by other researchers for uric acid biosensors but without an external mediator in the PBS solution, which was attributed to the integration of Ni microdiscs with a NiO matrix [Table 1].

Real sample analysis

As is well known, for a thorough evaluation of the analytical performance of the proposed method, the limit of detection, linearity, precision, stability, accuracy and selectivity need to be fulfilled by the prepared uricase/Ni/NiO/ITO/glass biosensor. Therefore, to demonstrate the practical feasibility of prepared uricase/Ni/NiO/ITO/glass biosensor for the analysis of uric acid in a real biological fluid, 10 human sera samples were analyzed and the % recovery and precision were calculated for spiked samples. After the addition of the sera samples in the electrolyte solution, the peak oxidation current values were noted from the CV measurements. The uric acid concentration (mM) in serum was then extrapolated from the standard calibration curve, and plotted as a function of the current (Fig. 6(d)). The electrochemical sensing technique in the present work was used to corroborate the results obtained from commercial spectrophotometric method in the clinical laboratory. To validate the accuracy, the content of uric acid in the serum samples determined by the prepared biosensor was compared with that measured by commercial spectrophotometric method in the clinical laboratory. Table 2 summarizes the results obtained during the present investigation. The results indicate that the uric acid analysis in sera with the developed biosensor agrees well with the spectrophotometric data. Recovery tests were also performed in order to demonstrate the accuracy and precision of the prepared biosensor by adding a known concentration of uric acid (0.50 mM) in the already tested serum samples and then estimating the concentration of added uric acid (Table 2). The performed recovery tests confirmed that the fabricated biosensor is accurate and precise. The performance of the prepared biosensor system was comparable to the commercially accepted methods. For the *in vivo* application of the biosensor in clinical practice, the requirements of biocompatibility, linearity, sensitivity, specificity, accuracy and long-term stability were fulfilled by the uricase/Ni/NiO/ITO based biosensor.

Conclusion

In summary, an efficient and reagentless uric acid biosensor was developed using a novel matrix of NiO thin film loaded with Ni microdiscs. Ni microdiscs distributed uniformly on the surface of NiO/ITO electrode provides an attractive platform for the effective immobilization of uricase using a physical adsorption technique. The activation of the Ni^{2+}/Ni^{3+} redox

couple in the matrix helps in the realization of a reagentless detection of uric acid as well as an enhanced sensing response. The prepared uricase/Ni/NiO/ITO bioelectrode exhibits high sensitivity (431.09 μA mM^{-1}), good linearity over a wide range of uric acid concentrations (0.05–1.00 mM), low value of K_m (0.15 mM) and a low detection limit (0.03 mM). The results obtained using a novel matrix of Ni microdiscs loaded NiO thin films are encouraging for the realization of an efficient uric acid biosensor.

Acknowledgements

Authors are thankful to the Department of Science and Technology (DST) and UGC for the financial support to carry out the proposed work. One of the authors (KA) acknowledges CSIR for fellowship.

References

1 K. Arora, M. Tomar and V. Gupta, *Biosens. Bioelectron.*, 2011, **30**, 333.
2 P. Schrenkhammer and O. S. Wolfbeis, *Biosens. Bioelectron.*, 2008, **24**, 994.
3 T. M. Pan, K. Y. Chang, C. W. Lin, S. W. Tsai and M. H. Wu, *Sens. Actuators, B*, 2011, **160**, 850.
4 R. Konck, T. Lenarczuk, A. Radomska and S. Glab, *Analyst*, 2001, **126**, 1080.
5 Z. Yang, S. Si, H. Dai and C. Zhang, *Biosens. Bioelectron.*, 2007, **22**, 3283.
6 T. Ahuja, Rajesh, D. Kumar, V. K. Tanwar, V. Sharma, N. Singh and A. M. Biradar, *Thin Solid Films*, 2010, **519**, 1128.
7 S. M. U. Ali, N. H. Alvia, Z. Ibupoto, O. Nur, M. Willander and B. Danielsson, *Sens. Actuators, B*, 2011, **152**, 241.
8 X. Wang, T. Hagiwara and S. Uchiyama, *Anal. Chim. Acta*, 2007, **587**, 41.
9 K. Arora, G. Sumanaa, V. Saxena, R. K. Gupta, S. K. Gupta, J. V. Yakhmi, M. K. Pandey, S. Chand and B. D. Malhotra, *Anal. Chim. Acta*, 2007, **594**, 17.
10 F. Zhang, X. Wang, S. Ai, Z. Sun, Q. Wan, Z. Zhu, Y. Xian, L. Jin and K. Yamamoto, *Anal. Chim. Acta*, 2004, **519**, 155.
11 S. P. Singh, S. K. Arya, P. Pandey, B. D. Malhotra, S. Saha, K. Sreenivas and V. Gupta, *Appl. Phys. Lett.*, 2007, **91**, 063901.
12 S. Saha, S. K. Arya, S. P. Singh, K. Sreenivas, B. D. Malhotra and V. Gupta, *Anal. Chim. Acta*, 2009, **653**, 212.
13 S. Saha and V. Gupta, *J. Appl. Phys.*, 2011, **110**, 064904.
14 A. Salimi, E. Sharifi, A. Noorbakhsh and S. Soltanian, *Biophys. Chem.*, 2007, **540**, 125.
15 W. D. Zang, C. Jin, J. L. Chuan, Y. Y. Xiang and Z. J. Qi, *Mikrochim. Acta*, 2010, **168**, 259.
16 A. Safavi, N. Maleki and E. Farjami, *Biosens. Bioelectron.*, 2009, **24**, 1655.
17 N. Sattarahmady, H. Heli and F. Faramarzi, *Talanta*, 2010, **82**, 1126.
18 H. Sato, T. Minami, S. Takata and T. Yamada, *Thin Solid Films*, 1993, **236**, 27.
19 M. Tyagi, M. Tomar and V. Gupta, *Anal. Chim. Acta*, 2012, **726**, 93.
20 Y. Liu, M. Yuan, L. Liu and R. Guo, *Sens. Actuators, B*, 2013, **176**, 592.
21 Y. Wang and Y. Hasebe, *J. Pharm. Biomed. Anal.s*, 2012, **57**, 125.
22 X. Liu, Y. Peng, X. Qua, S. Ai, R. Han and X. Zhu, *Electroanal. Chem.*, 2011, **654**, 72.
23 J. M. Zen, Y. Y. Lai, H. H. Yang and A. S. Kumar, *Sens. Actuators, B*, 2002, **84**, 237.
24 E. Miland and A. J. Miranda, *Talanta*, 1996, **43**, 785.
25 M. Hadi and A. Rouhollahi, *Anal. Chim. Acta*, 2012, **721**, 55.
26 Z. H. Sheng, X. Q. Zheng, J. Y. Xua, W. J. Bao, F. B. Wang and X. H. Xia, *Biosens. Bioelectron.*, 2012, **34**, 125.
27 R. M. A. Tehrani and S. A. Ghani, *Sens. Actuators, B*, 2010, **145**, 20.
28 S. Prakash, T. Chakrabarty, A. M. Rajesh and V. K. Shahi, *Measurement*, 2012, **45**, 500.
29 N. Chauhan and C. S. Pundir, *Anal. Biochem.*, 2011, **413**, 97.
30 S. B. Revin and S. A. John, *Bioelectrochemistry*, 2012, **88**, 22.
31 H. Chu, X. Wei, M. Wu, J. Yan and Y. Tu, *Sens. Actuators, B*, 2012, **163**, 247.
32 J. Arora, S. Nandwani, M. Bhambi and C. S. Pundir, *Anal. Chim. Acta*, 2009, **647**, 195.
33 P. Y. Chen, R. Vittal, P. C. Nien, G. S. Liou and K. C. Ho, *Talanta*, 2010, **80**, 1145.
34 Y. C. Luo, J. S. Do and C. C. Liu, *Biosens. Bioelectron.*, 2006, **22**, 482.
35 D. M. Perez, M. L. Ferrer and C. R. Mateo, *Anal. Biochem.*, 2003, **322**, 238.
36 R. Rawal, S. Chawla, N. Chauhan, T. Dahiya and C. S. Pundir, *Int. J. Biol. Macromol.*, 2012, **50**, 112.
37 S. Behera and C. R. Raj, *Biosens. Bioelectron.*, 2007, **23**, 556.

